Ozone and Aerosol Changes During the 1991–1992 Airborne Arctic Stratospheric Expedition

Edward V. Browell,* Carolyn F. Butler, Marta A. Fenn, William B. Grant, Syed Ismail, Mark R. Schoeberl, Owen B. Toon, Max Loewenstein, James R. Podolske

Stratospheric ozone and aerosol distributions were measured across the wintertime Arctic vortex from January to March 1992 with an airborne lidar system as part of the 1992 Airborne Arctic Stratospheric Expedition (AASE II). Aerosols from the Mount Pinatubo eruption were found outside and inside the vortex with distinctly different distributions that clearly identified the dynamics of the vortex. Changes in aerosols inside the vortex indicated advection of air from outside to inside the vortex below 16 kilometers. No polar stratospheric clouds were observed and no evidence was found for frozen volcanic aerosols inside the vortex. Between January and March, ozone depletion was observed inside the vortex from 14 to 20 kilometers with a maximum average loss of about 23 percent near 18 kilometers.

During the winter of 1988–1989, the first Airborne Arctic Stratospheric Expedition (AASE I) was conducted, the results of which established that the same chlorine-related chemistry that was responsible for O_3 depletion in the springtime Antarctic stratosphere was also occurring in the wintertime Arctic stratosphere (*1*). A second AASE campaign (AASE II) was then conducted during the winter of 1991–1992 to study the evolution of the dynamics, chemistry, and O_3 depletion associated with the wintertime Arctic vortex. In both of these expeditions, an airborne differential absorption lidar (DIAL) system (*2–4*) was flown on a DC-8 aircraft to make measurements of O_3 and aerosol profiles from ~1 km above the aircraft to altitudes of 23 to 26 km for O_3 (*5*) and to about 26 km for aerosols (*6*). In this report, we describe the results of observations of aerosols and O_3 in the wintertime Arctic stratosphere from January to March 1992 and the implications of the data for understanding atmospheric dynamics and chemical O_3 loss in the Northern Hemisphere.

The airborne DIAL system simultaneously transmits six laser beams at ~10 Hz directly above the DC-8 for profile measurements of O_3 concentrations and aerosol backscatter and depolarization in the lower stratosphere. The DIAL O_3 measurements are taken with the use of on- and off-line DIAL wavelengths of 301.5 and 311 nm, respectively (*2–5*, *7*). Two orthogonally polarized beams at 603 and 1064 nm are used to measure the atmospheric backscatter and depolarization (*2–4*, *6–8*). Measurements were obtained from January to March 1992 on long-range flights made each month from the National Aeronautics and Space Administration (NASA) Ames Research Center (ARC) in Moffett Field, California, to Anchorage, Alaska, to Stavanger, Norway, to Bangor, Maine, and then back to NASA ARC. Additional flights into the vortex were made each month from either Stavanger or Bangor, depending on the location of the vortex. Each flight lasted ~10 hours and covered ~8000 km. The DC-8 deployment periods were 14 to 23 January, 12 to 22 February, and 10 to 20 March 1992. An average of five high-latitude flights was made in each period, and at least three flights in each period went across a part of the Arctic vortex.

The lidar return from the atmosphere is calibrated to determine the atmospheric scattering ratio (R_T) at a specific altitude, where R_T is defined as the sum of the aerosol and molecular scattering divided by the molecular scattering (*6*, *9*). The value of R_T is calculated at both the 603-nm [visible (VIS)] and 1064-nm [infrared (IR)] lidar wavelengths (*10*). The aerosol scattering ratio R_A can also be calculated from R_T with the relation $R_A = R_T - 1$. The atmospheric depolarization was also measured at 603 and 1064 nm with two orthogonally polarized lidar returns at each wavelength (*11*). The total atmospheric depolarization (D_T) is defined as the perpendicular backscattered return (S_S) divided by the parallel return (S_P), or $D_T = S_S/S_P$ (*12*). The aerosol depolarization (D_A) can also be determined from the relation $D_A = (S_S - M_S)/(S_P - M_P)$, where M_S and M_P are the perpendicular and parallel molecular returns, respectively (*6*, *13*).

The airborne lidar measurements of O_3 profiles in the lower stratosphere were made through the DIAL technique with a correction for errors created by aerosol backscatter

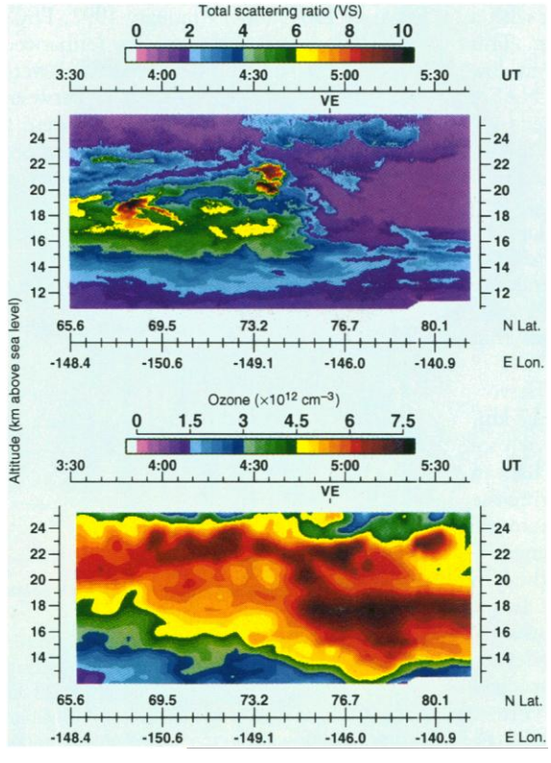

Fig. 1. Airborne lidar measurements of (**top**) aerosol and (**bottom**) O_3 distributions from outside to inside the Arctic vortex on a long-range flight from Anchorage, Alaska, to Stavanger, Norway, on 16 January 1992. The total atmospheric scattering ratios at 603 nm and O_3 concentrations are presented according to the color scales at the top of their respective figures. The vortex edge (VE), as defined by the *PV* analysis on the 440 K surface, is noted on the figure. Abbreviations: VS, visible scattering; UT, universal time; Lat., latitude; Lon., longitude.

E. V. Browell, W. B. Grant, S. Ismail, Atmospheric Sciences Division, NASA Langley Research Center, Hampton, VA 23681.
C. F. Butler and M. A. Fenn, Science Applications International Corporation, Hampton, VA 23666.
M. R. Schoeberl, NASA Goddard Space Flight Center, Greenbelt, MD 20771.
O. B. Toon, M. Loewenstein, J. R. Podolske, NASA Ames Research Center, Moffett Field, CA 94035.
*To whom correspondence should be addressed.

effects. A Bernoulli aerosol correction technique (*3*, *14*) was used with a normalized aerosol phase function of 0.028 sr^{-1} at 311 nm and an aerosol backscatter wavelength dependence of 0.7 between 301.5 and 311 nm (*15*). The uncertainty of the DIAL O_3 measurements in the presence of aerosol layers has been shown to be less than 10% under a wide range of aerosol conditions in the troposphere and stratosphere (*2–5*, *7*, *14*, *16*). On the basis of many comparisons between DIAL and ozonesonde measurements inside and outside the vortex during AASE II, it was estimated that the accuracy of the DIAL O_3 measurements was better than 5% under conditions of low solar background. The O_3 mixing ratio profile was determined from the DIAL-derived O_3 concentration profile by division of the O_3 number density at each altitude by the molecular number density derived from the closest 12-hour National Meteorological Center (NMC) meteorological analysis for the same location (*17*).

Aerosols from the Mount Pinatubo eruption in June 1991 were observed in the stratosphere across the entire Arctic region throughout the AASE II campaign (Fig. 1). The vortex edge was defined dynamically where the potential vorticity (PV) has the largest gradient on a potential temperature (Θ) surface. This location is usually close to where PV = $\sim 2.5 \times 10^{-5}$ cm^2 K g^{-1} s^{-1} on the 440 K ($\sim$17 km) potential temperature surface (*18*). On all flights the aerosol scattering declined dramatically above $\sim$15 km across the vortex edge. Outside the vortex, the Mount Pinatubo aerosols extended from below 11 km to 26 km with a January R_T value of 5.3 at 18 km. This value is about half that observed at low latitudes (5° to 20°N) during the NASA Pacific Exploratory Mission conducted over the western Pacific from September to October 1991. The average ratio of the IR to VIS aerosol scattering ratios ($R_{IR/VIS}$) was $\sim$2.2 at the peak of the Pinatubo layer at both low latitudes and outside the Arctic vortex. This ratio represents a dependence of aerosol backscatter on wavelength (α in $\lambda^{-\alpha}$) of $\sim$2.6, indicative of aerosols that are $\sim$1 μm in diameter.

The aerosol distribution inside the vortex (Fig. 1) extended from $\sim$12 to 17 km. The maximum scattering of the aerosol layer in the vortex during January had an R_T (VIS) value of 2.9 at 15 km. During the 1989 AASE I campaign, the background stratospheric aerosols were also generally below 18 km inside the vortex, and the VIS scattering ratio was less than 1.2 (6). Inside the vortex during AASE II, $R_{IR/VIS}$ was $\sim$2 and the backscatter wavelength dependence, and hence the particle size, was similar to that found outside the vortex. These values indicate that although the nature of the aerosols is the same, the amount of Pinatubo aerosols that reached the Arctic before the establishment of the vortex in the fall of 1991 was clearly less than the amount that was observed outside the vortex in January 1992.

Throughout the campaign, aerosol depolarization was consistently low (<1.3%) across the main part of the Pinatubo layer above 16 km outside the vortex and above 14 km inside the vortex. This low depolarization is consistent with the small and nearly spherical sulfuric acid aerosols that dominate the composition of the Pinatubo layer. No evidence was found of frozen sulfuric acid aerosols within the vortex. Aerosol depolarization was higher (2 to 6%) at the bottom of the Pinatubo layer (generally below 14 km), where the aerosol scattering ratios were low (<2) both inside and outside the vortex. The high depolarization and low scattering are associated with the low density of nonspherical aerosols that resulted from the subsidence of volcanic ash particles. Direct collection of particles at DC-8 altitudes, where lidar depolarization was observed, showed that ash particles were present (*19*).

No polar stratospheric clouds (PSCs) were observed from the DC-8 inside the vortex during AASE II. This absence was generally indicative of the warmer temperatures (≥195 K) seen in the NMC analysis during the winter of 1991–1992 compared to those of the colder winter of 1988–1989, when PSCs were observed during AASE I on 10 of 11 flights from 6 January to 2 February 1989. On 19 January 1992, PSCs with the properties of water ice (enhanced aerosol scattering and depolarization) were observed just outside the vortex between Norway and Iceland in a region where a tropospheric high-pressure system forced the air in the upper troposphere and lower stratosphere to rise by several kilometers and to cool adiabatically to temperatures below 195 K (*20*, *21*). Toon and colleagues (*20*) propose that these aerosols were frozen volcanic aerosols containing substantial dissolved HNO_3.

A sharp decrease in the altitude of the O_3 distribution was observed upon entrance into the Arctic vortex on all flights (Fig. 1). The peak O_3 concentration outside the vortex was $\sim 6 \times 10^{12}$ cm^{-3} at 22 km, whereas inside the vortex about the same concentration was observed at $\sim$17 km. The decrease in altitude of the O_3 distribution inside the vortex results from the descent that occurs there during the winter as a consequence of diabatic cooling. The location of the vortex edge determined from the O_3 distribution corresponds closely with the location derived from the aerosol distribution and the NMC PV analysis. In addition, there are small-scale features seen in the O_3 and aerosol distributions that are not reflected in the lower resolution NMC analysis of PV.

Air parcels are advected along Θ surfaces, and the mixing ratio of O_3 is conserved in the absence of diabatic processes, which alter Θ, and chemical processes, which alter O_3. Thus, to separate transport and chemical processes, the O_3 mixing ratio distributions must be examined against Θ. Aerosol scattering ratios must also be examined against Θ to assess transport processes and aerosol-O_3 relation. During January, the potential temperature surfaces below 575 K inside the vortex were higher in altitude than outside it; for example, on the 400 K Θ surface, the altitude difference was 950 m. For all missions, the O_3 mixing ratio profiles were calculated from the O_3 concentration profiles and plotted against Θ by the use of the NMC analysis. The O_3 mixing ratio profiles outside the vortex were found to increase with altitude to a maximum at 640 K in January. The edge of the vortex below 500 K was also readily identified in the O_3 mixing ratio–Θ distribution by the location of the maximum horizontal

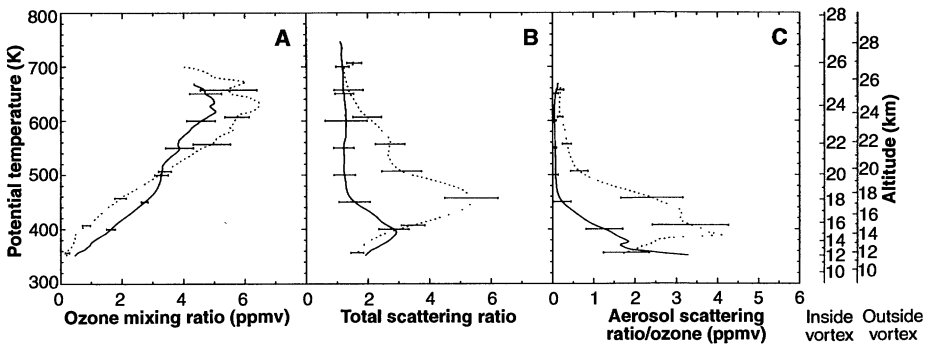

Fig. 2. January profiles of (**A**) average O_3 mixing ratios, (**B**) total atmospheric scattering ratios, and (**C**) ratios of aerosol scattering to O_3 for inside (solid line) and outside (dashed line) the vortex. Data from five flights during the period of 14 to 23 January 1992 were used in these average profiles. The horizontal bars represent the standard deviation of the measurements inside and outside the vortex. Average altitude reference scales are given on the right for conditions inside and outside the vortex.

O_3 gradient on a Θ surface.

To obtain average O_3 and aerosol profiles inside and outside the vortex, we binned the data from all flights during a month on the basis of the *PV* analysis. We assumed that measurements were inside the vortex when PV ≥ 2.75×10^{-5} cm^2 K km^{-1} s^{-1} on the 440 K Θ surface and outside the vortex when PV was in the range of 1.25×10^{-5} to 1.75×10^{-5} cm^2 K km^{-1} s^{-1}. At Θ levels below 500 K (Fig. 2), the O_3 mixing ratio was higher inside the vortex than outside it, whereas above this the reverse was true (*22*). This O_3 difference at the same Θ (Fig. 2) could result from diabatic cooling altering Θ and from the chemical loss of O_3. These effects must be separated to determine the magnitude of the chemical loss. For example, below the 500 K level, the transport of extra-vortex air into the vortex would appear as an O_3 loss because the extra-vortex air has less O_3 than does the vortex air at the same Θ level. The average scattering ratio profiles in January (Fig. 2) indicate that the change in aerosol characteristics across the vortex edge shown in Fig. 1 were representative of the general conditions inside and outside the vortex on all flights in January. Outside the vortex significant aerosol loading extended from 350 K (11.4 km) to 680 K (~26 km), whereas inside the vortex nearly all of the aerosols were below 450 K (18 km). The scattering ratios inside the vortex below 400 K were higher than that outside the vortex because the aerosols inside the vortex were concentrated on slightly lower Θ surfaces (~20 K lower).

The ratio of the aerosol scattering ratio to the O_3 mixing ratio can be used as a tracer of horizontally transported air because the aerosols and O_3 would be transported together and their ratio should be conserved over short time scales (days to weeks). Above 380 K (~14 km), this relation inside the vortex is different from that outside, and this difference can be used to identify air being transported into or out of the vortex. Below 380 K, the variability in the relation cannot be relied on to identify the air being transported. Similar profiles were also found for February and March. These relations were used to identify cases of intrusions of extra-vortex air with low *PV* into the vortex (*23*) and cases in which the *PV* analysis did not accurately identify the edge of the vortex.

The peak aerosol scattering (R_A) outside the vortex increased by 45% between January and February and remained relatively unchanged into March. Inside the vortex the peak R_A value increased by 108% over the same period (Fig. 3). The top of the aerosol distribution inside the vortex (defined where R_T = 2.0) increased in altitude from 17 km at 435 K to 18.2 km at 470 K. The value of R_T at 603 nm increased from a sharp peak of 2.9 at 395 K (15 km) to a broad peak of ~5.0 centered at 382 K (13.4 km). These changes indicate that horizontal transport began eroding the vortex primarily below 430 K. During the intrusion of air from outside the vortex into this region, the vortex can become greatly distorted. However, the aerosol and O_3 measurements inside the vortex for February and March 1992 showed that above 17.8 km (465 K), these intrusions were not irreversibly mixed into the high-PV region (PV ≥ 2.75×10^{-5} cm^2 K km^{-1} s^{-1}) of the vortex.

Inside the vortex, the average O_3 in February was lower in the 400 to 500 K (14 to 20 km) region than in January, with a maximum decrease of ~10% at 460 K (18 km in February) (Fig. 4). The changes in O_3 above 450 K were uncorrelated with the Pinatubo aerosols. Above 500 K, the O_3 differences between January and February were not significant. The radiative cooling of air inside the vortex during the winter results in the diabatic descent of air to lower Θ surfaces. Between January and February the amount of diabatic descent decreased from 30 K at Θ of 500 K to 14 K at Θ of 400 K (*24*). In consideration of this additional difference between the starting and ending Θ levels, the amount of O_3 loss was determined by the comparison of the February O_3 profile with the descended January reference O_3 profile. The acutal O_3 loss at 460 K was 18%, and the O_3 loss decreased to 11% at 500 K. The transport of extra-vortex air into the lower vortex, primarily below 430 K, can account for a significant portion of the O_3 decrease in that region. The average O_3 depletion between January and February 1992 was similar to the amount observed inside the vortex in February 1989 (17%). However, in 1989 the region of maximum O_3 loss was at 500 K and extended to 580 K (*5*).

The average O_3 profile inside the vortex in March 1992 was similar to the average February profile. The diabatic descent between February and March decreased from ~20 K at 500 K to 5 K at 400 K (*24*), and the amount of additional O_3 change during this period was limited to ~5% at 460 K, with most of the larger changes at the lower altitudes being dominated by transport. The maximum average O_3 depletion from January to March 1992 inside the vortex was ~23% near 460 K. The unusually warm stratospheric temperatures in the Arctic during the winter of 1991–1992 produced fewer PSCs than in previous years (*25*), which in turn reduced the amount of O_3 depletion that was observed during AASE II.

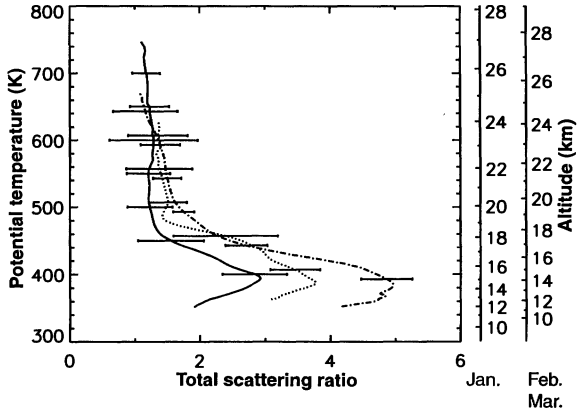

Fig. 3. Profiles of the average total scattering ratio inside the Arctic vortex for January (solid line), February (dotted line), and March (dotted and dashed line) 1992. The horizontal bars represent the standard deviation of the measurements inside the vortex. Reference altitude scales are shown on the right side of the figure (Jan., January; Feb., February; and Mar., March).

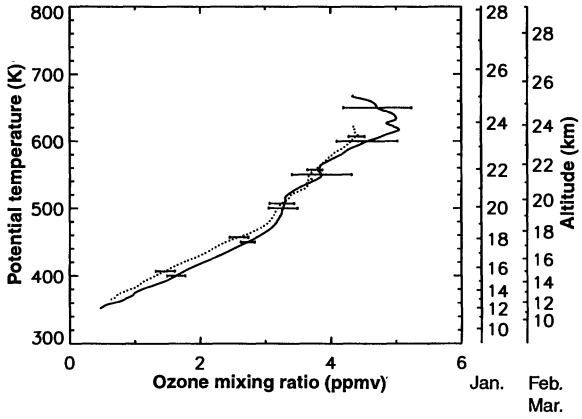

Fig. 4. Comparison of average O_3 profiles obtained inside the vortex during the periods of 14 to 23 January (solid trace) and February (dashed trace) 1992. The horizontal bars represent the standard deviation of the measurements inside the vortex, which are <10% below 500 K, and the standard error of the average profiles below 500 K is ≤1%.

REFERENCES AND NOTES

1. R. Turco, A. Plumb, E. Condon, *Geophys. Res. Lett.* **17**, 313 (1990).
2. E. V. Browell *et al.*, *Appl. Opt.* **22**, 522 (1983).
3. E. V. Browell, *Proc. IEEE* **77**, 419 (1989).
4. _____, *Opt. Photonics News* **2**, 8 (1991).
5. E. V. Browell *et al.*, *Geophys. Res. Lett.* **17**, 325 (1990).
6. E. V. Browell *et al.*, *ibid.*, p. 385.
7. E. V. Browell *et al.*, in "Polar Ozone Workshop," *NASA Conf. Publ. CP-10014* (1988), pp. 61–63.
8. The visible depolarization was measured from the parallel backscatter component at 603 nm and the perpendicular backscatter component at 622 nm. These wavelengths were generated from the lasers used in the DIAL system. The relative error in the aerosol depolarization measurement at 603 nm from the use of the 622-nm wavelength for the perpendicular component is expected to be less than 5%.
9. For the determination of the atmospheric scattering ratio profile, the relative molecular scattering profile needs to be determined for each observation. To do so, a clean (aerosol-free) region for each flight is identified along the flight track at an altitude above ~18 km that has a signal-to-noise ratio sufficient for an accurate estimate of the molecular scattering. The relative molecular scattering profile is then calculated by the normalization of the molecular number density profile from the NMC meteorological analysis to the relative scattering in the clean region. The relative molecular scattering profile at any other location is then calculated with the molecular number density profile at the new location, the molecular scattering normalization obtained in the clean region, and the relative change in the laser energy or other lidar system parameters from the normalization location. The lidar backscatter return from the atmosphere is then divided by the derived return of molecular lidar backscatter to get R_T.
10. In this analysis, it is assumed that extinction of the lidar signal due to atmospheric scattering and absorption is negligibly small.
11. The lidar returns in each polarization were obtained within 300 μs, and one detector system for each wavelength was used to detect both the parallel and perpendicular backscattered returns.
12. When the atmosphere has a small amount of aerosol scattering compared to molecular scattering, the total atmospheric depolarization reflects more depolarization from the molecules than from the aerosols.
13. The perpendicular and parallel molecular returns can be determined with the same normalization technique described for the determination of the atmospheric scattering ratio distribution (*9*).
14. E. V. Browell, S. Ismail, S. T. Shipley, *Appl. Opt.* **24**, 2827 (1985).
15. These parameters were determined after extensive sensitivity analyses were conducted to minimize aerosol backscatter effects in the DIAL measurement (*3, 14*). The Bernoulli technique was normalized in the far field (above the Pinatubo aerosols) to a scattering ratio of 1.0 for the O_3 DIAL off-line wavelength (311 nm). The aerosol backscatter distribution at 311 nm was determined through this technique. The dependence of aerosol backscatter on wavelength between 301.5 and 311 nm was determined by an analysis of the wavelength dependence of backscatter with the use of combinations of 311-, 603-, and 1064-nm lidar returns, and the results were tested in regions of high aerosol structure. The backscatter wavelength-dependent errors were typically ≤15% outside and ≤5% inside the vortex. After application of the above correction technique, the remaining residual errors in the DIAL-derived O_3 profiles were ≤5% outside and ≤2% inside the vortex.
16. J. Margitan *et al.*, *J. Geophys. Res.* **94**, 16557 (1989).
17. Because the O_3 mixing ratio is conserved in adiabatic processes, it is the preferred quantity for the examination of isentropic O_3 transport and changes in O_3 due to chemical processes.
18. The vortex edge is not a well-defined boundary, and because it varies with altitude the general region from 430 to 530 UT in Fig. 1 may be considered a transition or edge region.
19. R. Pueschel, unpublished results.
20. O. B. Toon *et al.*, *Science* **261**, 1136 (1993).
21. The cooling of the vertically displaced air, which contained Pinatubo aerosols, caused the aerosols to grow in size by the adsorption of H_2O vapor and HNO_3 vapor, which increased the scattering ratio of the aerosols by at least a factor of 2. In a cold region (~191 K) near the top of the Pinatubo layer (~21 km), the aerosols had greatly enhanced aerosol scattering [maximum R_A (VIS) ~40 and R_A (IR) ~165] and enhanced depolorization (D_A > 25%) (*20*). The backscatter wavelength dependence was calculated to be 1.5, which indicates that these nonspherical aerosols have a volume equivalent radius of <1 μm (*20*). The scattering and depolarization of these aerosols are similar to the Type II H_2O ice PSCs (*6*); however, their size is generally smaller, which could be due to the rapid cooling of the air passing through the uplifted region.
22. The altitude of the 500 K level was nearly the same inside (20 km) and outside (19.5 km) the vortex.
23. R. A. Plumb, D. W. Waugh, P. A. Newman, L. R. Lait, M. R. Schoeberl, *Eos* **73**, 115 (1992).
24. Diabatic descent was determined from the combination of in situ aircraft and balloon measurements of N_2O distributions (J. R. Podolske, M. Loewenstein, A. Weaver, K. R. Chan, S. E. Strahan, *ibid.*, p. 98; U. Schmidt, R. Bauer, A. Engel, C. Schiller, R. Borchers, *ibid.*, p. 106) and from modeling studies.
25. P. A. Newman *et al.*, *Science* **261**, 1143 (1993).

26. We thank N. S. Higdon, M. L. Jones, M. N. Mayo, W. J. McCabe, B. L. Meadows, and J. A. Williams for their assistance in developing and operating the airborne DIAL system and G. D. Nowicki, S. D. Mayor, and S. A. Kooi for assistance in reducing the lidar data and producing the color data plots. Supported by NASA's Upper Atmospheric Research Program.

19 February 1993; accepted 13 July 1993